

Green Synthesis, Characterization and Antibacterial Activities of Silk Sericin Capped Zinc Oxide Nanoparticles

Aleyna TEMEL ¹, Zehra GÜN GÖK ¹

¹ Kırıkkale Üniversitesi, Mühendislik ve Doğa Bilimleri Fakültesi, Biyomühendislik Bölümü, Kırıkkale, Türkiye

Abstract

In recent years, interest in metal-based antibacterial materials has increased due to microorganisms gaining resistance to antibiotics. Silk sericin obtained from *Bombyx mori* cocoon has found use in many different areas thanks to its biocompatibility, hydrophilic character and biodegradability. Zinc oxide nanoparticles (ZnONPs) obtained in various zinc salts exhibit broad-spectrum antibacterial properties. In this study, to be produce metal based antibacterial materials, synthesis of silk sericin-coated ZnONPs (SS-ZnONPs) in a green and scalable method was investigated by using silk sericin protein as both reducing and capping agent to obtain ZnONPs. For producing SS-ZnONPs, 2% silk sericin solution was mixed with Zn(NO₃)₂ solution and the blend solution was heated at 100 °C for a certain period of time. Observing surface plasmon resonance (SPR) peak specific at 380 nm in the UV-vis spectrum of SS-ZnONPs represented the formation of ZnONPs. Then, the chemical, morphological, crystalline, thermal, and antibacterial properties of the synthesized SS-ZnONPs were examined. Characteristic peak of the Zn-O band was found in fourier transform infrared spectroscopy (FTIR) analysis of SS-ZnONPs. According to scanning electron microscopy (SEM) analyses, ZnONPs had morphology similar to cubic/hexagonal shape, showed a uniform structure, and did not represent any agglomerations. In energy dispersive spectroscopy (EDS) analyses of SS-ZnONPs, peaks belonging to carbon, nitrogen, oxygen, sulphur, and zinc elements were observed. The formation of Zn peak indicated that the zinc ions were transformed into ZnONPs. In addition, characteristic peaks of zinc were seen in the X-ray diffractometer (XRD) result of SS-ZnONPs. Thermogravimetric analysis (TGA) showed that the thermal stability and remaining amount of SS-ZnONPs was higher compared to pure silk sericin powder due to the formation of ZnONPs. Lastly, agar well diffusion test was carried out with *Staphylococcus aureus* (ATCC 6538) and *Escherichia coli* (ATCC 25922) bacteria and SS-ZnONPs showed antibacterial action against *S. aureus*. It has been observed that the obtained SS-ZnONPs can be used as antibacterial agents. However, it was also understood that the ZnONPs concentration in this study was low for high antibacterial activity.

Keywords: Green synthesis, Silk sericin, Zinc oxide nanoparticles, Antibacterial materials

I. INTRODUCTION

Nanoparticles (NPs) are atomic level particles having 1-100 nm size and they can be produced from a wide variety of materials. NPs are categorized as metallic NPs (for example; Ag, Zn and Au), metal and non-metal oxides NPs (for example; ZnO, FeO and AlO); semiconductor NPs (for example; CdS, ZnS and ZnSe) and carbon NPs [1,2]. Compared to bulk materials, NPs have different advanced features in size, distribution and morphology [3]. The quantum effect, surface and heterogeneity of NPs play a significant role in the chemical reactivity, optical, mechanical, electrical and even magnetic features of NPs. Heterogeneity and surface area of NPs can also affect other properties such as antimicrobial activity [2,3].

In the field of nanotechnology, there have been spectacular developments in recent years, with various advanced methodologies to synthesize NPs of certain forms and sizes. NPs can be obtained by physical, chemical and biological and green procedures. Various physical and chemical techniques such as sol-gel synthesis, laser ablation, hydrothermal and lithography have been developed. However, these methods may have disadvantages such as requiring special equipment and skilled labour, and may have toxic effects due to the use of harmful chemicals [4]. Increasing demands for environmentally friendly NPs have increased the interest in obtaining NPs with green synthesis methods instead of physical and chemical methods [5]. Many metal and metal oxide NPs have been synthesized by green synthesis methods, by using natural molecules as both stabilizing and reducing agents [5-7].

One of the excellent metallic nanomaterials is zinc NPs (ZnNPs) and ZnONPs. Zinc is a highly active element and also a powerful reducing agent [8]. Zinc is one of the most essential microelements in human beings and is existed in all of tissues, especially muscle, skin and bone [2,9,10]. ZnONPs are obtained from zinc salts by various methods such as chemical or chemical vapor deposition, hydrothermal synthesis technique, laser vaporization condensation technique, precipitation and green synthesis technique [13]. ZnONPs have a wide range of usages areas in different industrial areas [2,11]. With wide band gap (3.37 eV), ZnO has good transparency at room temperature and it is used as semiconductor materials [11,12]. Due to the strong pharmacological properties of ZnO, ZnONPs has usage areas in health fields as an anticancer, antimicrobial and antioxidant agent [2,11]. Additionally, ZnONPs are less toxic to the human body compared to other NPs and Zn ions, which are the dissolved form of ZnO, are substances found in normal human physiological system [13].

Silk cocoons are formed two main proteins called sericin and fibroin [14]. Fibroin is a fibrous protein that forms the structure of the cocoon and has been used for years in different application areas [15]. On the other hand, sericin is a globular water-soluble protein that keeps the fibroin proteins in the cocoon together. Sericin has 18 distinct amino acids in its structure and mostly contains amino acids containing polar groups [14]. After obtaining fibroin in silk processing plants, the sericin protein is disposed of together with the wastewater. However, sericin is a cheap, readily available, biodegradable and biocompatible material [5,7]. Many valuable biological activities of silk sericin have been reported in the literature and silk sericin has wide applications areas in tissue engineering [16,17], wound healing material synthesis [18,19], drug delivery [20,21], cosmetics [22,23] and food additives [24]. After the studies showing the usability of sericin in these important areas, many researchers continue to make new studies on sericin. Although sericin is mostly used in the production of wound dressing materials due to its increase in cell proliferation and biocompatibility, it is a protein with different uses, such as a reducing agent in the production of various NPs [25-28], in the synthesis of packaging materials [29] and in the production of adsorbent materials [30].

There are a few studies in the literature using sericin protein for ZnONPs synthesis [8,31]. However, to our knowledge, there is no study in the literature on the production of stable ZnONPs using only silk sericin as reducing and stabilizing material. However, in these studies, sericin protein was not used alone as a reducing and coating agent. In the current our study, stable ZnONPs were obtained by a simple, green method using only silk sericin solution as reducing and stabilizing agent and the chemical, morphological,

thermal and antibacterial properties of the obtained SS-ZnONPs were investigated.

II. MATERIALS AND METHODS

2.1. Materials

Silk sericin in solid powder form (obtained from *Bombyx mori* silkworm, CAS no. 60650-88-6; 60650-89-7, MA: ca. 138 kDa) was taken from Nembri Industrie Tessili. All other chemical and the bacterial cultures mediums were supplied from Merck (Germany) and Across Bio, respectively.

2.2. Synthesis of SS-ZnONPs

Silk sericin and zinc solutions were prepared for the obtaining of SS-ZnONPs. To prepare sericin solution, 2 grams of sericin were taken and added to 100 mL of water. After heating the mixture, pH of sericin mixture was raised to above 7 with NaOH, ensuring complete dissolution of sericin [5]. Then, the prepared 10 mM $Zn(NO_3)_2$ solution (30 mL) was added to the boiling silk sericin solution (30 mL) in a controlled manner. When $Zn(NO_3)_2$ were added to the silk sericin solution, a white-cloud-like solution was formed. The mixture was heated in a controlled manner for 2 hours and in continuation, it was stirred for 24 hours at room temperature. For FTIR, XRD, SEM-EDS analyses, liquid mixture of SS-ZnONPs was poured into petri dishes and the mixture was dried in an oven (50 °C, 1 day). Finally, powders of SS-ZnONPs were collected as solids from petri dishes.

2.3. Characterization of SS-ZnONPs

With a UV-Vis spectrophotometer (Biochrom, UK), UV-Vis absorption spectra of SS-ZnONPs solution was measured between 300 and 500 nm wavelength range. For chemical characterization of SS-ZnONPs, the FTIR spectra of the silk sericin and SS-ZnONPs were obtained with a FTIR device (Bruker Vertex 70 V). The morphologies and elemental analysis of the SS-ZnONPs were investigated with a SEM device and EDS analysed were obtained on SEM images (QUANTA 400F Field Emission SEM). After mixing the SS-ZnONPs homogeneously, with a ZetaSizer instrument (Malvern Instruments, Malvern, UK), the zeta size and potential of the SS-ZnONPs were recorded. The crystal structure of SS-ZnONPs was examined with a XRD device (Rigaku Ultima-IV brand) in the 0-80° scanning range. The thermal properties of SS-ZnONPs and original silk sericin were determined by TGA (PerkinElmer) between 25-950 °C with 10 °C/min heating rate.

2.4. Evaluation of Antibacterial Properties of SS-ZnONPs

Agar well diffusion test procedure was carried out in solid medium by using *E. coli* and *S. aureus* bacteria according to our previous works [5,7,32]. For the test, liquid cultures of *E. coli* and *S. aureus* bacteria were prepared and the number of cells in cell suspensions for bacterial cultures was adjusted to 10^8

microorganisms/mL by measuring optical densities of the bacterial cultures. 100 μL bacterial samples from these suspensions were poured to Mueller Hinton agar plate (prepared in 20 mm petri dish) and the cells were spread over the entire surface with sterile cotton swab. After 10 minutes of bacterial plating, wells were opened in solid media with 7 mm diameter with 1 mL pipette tip back on each agar surfaces. 100 μL of SS-ZnONPs samples (sterilized by keeping under UV-light at 254 nm in a cabinet for 1 hour) were placed to the opened wells and the petri dishes were incubated for 24 hours at 37 $^{\circ}\text{C}$. For the antibacterial test performed, autoclave sterilized water and gentamicin antibiotic discs were used as negative and positive control, respectively. After 24 hours of incubation, it was checked whether there were inhibition zone areas around the wells and the resulting inhibition zone diameters were measured with the help of a ruler.

III. RESULTS AND DISCUSSION

3.1. Production of SS-ZnONPs

For production of SS-ZnONPs, solutions of silk sericin and $\text{Zn}(\text{NO}_3)_2$ were blended and solution of sericin- $\text{Zn}(\text{NO}_3)_2$ was heated at 100 $^{\circ}\text{C}$ after NaOH addition (Figure 1). As time passed, sericin- $\text{Zn}(\text{NO}_3)_2$ solution colour turned from yellow to cloudy white. The occurrence of color change was proof that silk sericin converted zinc ions to ZnONPs. Because, sericin can reduce the zinc ions to ZnONPs due to its functional groups found its structure. This color change observed due to ZnO formation has been reported in many studies in the literature [33,34].

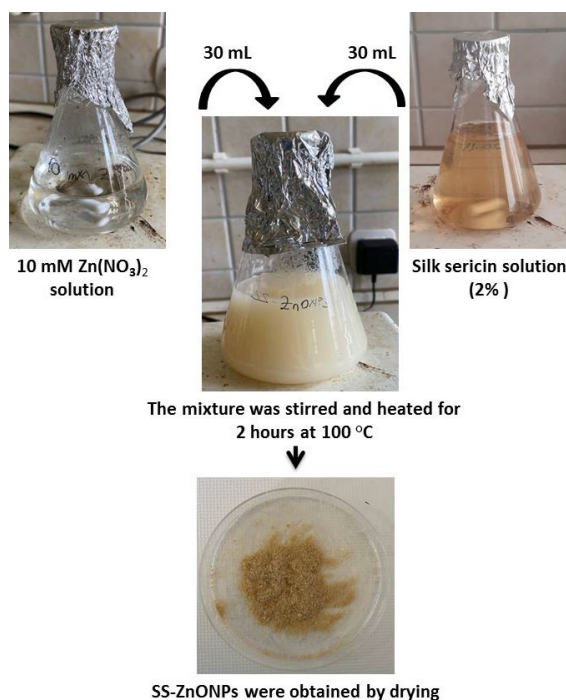


Figure 1: Obtaining SS-ZnONPs with silk sericin solution

Afterwards, the absorbances of solutions of silk sericin, $\text{Zn}(\text{NO}_3)_2$ SS-ZnONPs were recorded between 300-500 nm and the results were given in Figure 2. SPR peak specific to ZnONPs around 380 nm was observed while $\text{Zn}(\text{NO}_3)_2$ and sericin solution did not show any SPR peak. There are many studies in the literature showing that ZnONPs have SPR peaks in the range of approximately 350-400 nm [35,36]. This peak formation represent formation of hexagonal wurtzite ZnO and according to the literature, the result we obtained was compatible [37,38].

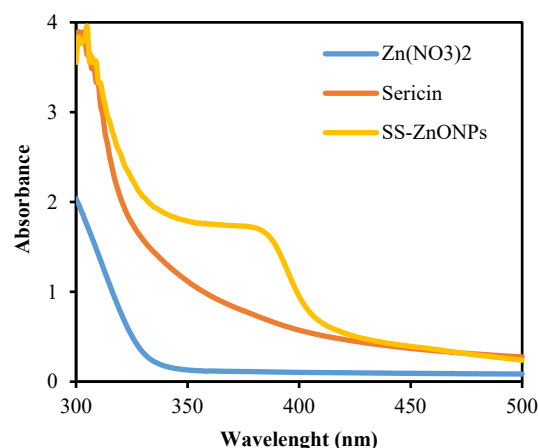


Figure 2: UV-Vis analyses of $\text{Zn}(\text{NO}_3)_2$, silk sericin, and SS-ZnONPs sample between 300-500 nm

3.2. Characterization of SS-ZnONPs

For the SS-ZnONPs samples, zeta size and zeta potential was found as 316.4 and -22.4 mV, respectively (Figure 3 (a) and 3(b)). The zeta potentials of the synthesized SS-ZnONPs were found to be negative. This result shows that the synthesized SS-ZnONPs were stable and had homodispersed distribution since the negatively charged ZnONPs repelled each other in aqueous solution [32,39]. The fact that NPs had a negative zeta potential is because of the use of sericin protein as a coating agent. Because, ZnONPs were synthesized at a pH that was above the isoelectric point of the sericin (isoelectric point of silk sericin is 3.7) [5]. When we look at the zeta size distribution plot of the synthesized NPs, it was seen that the ZnONPs have different size distributions.

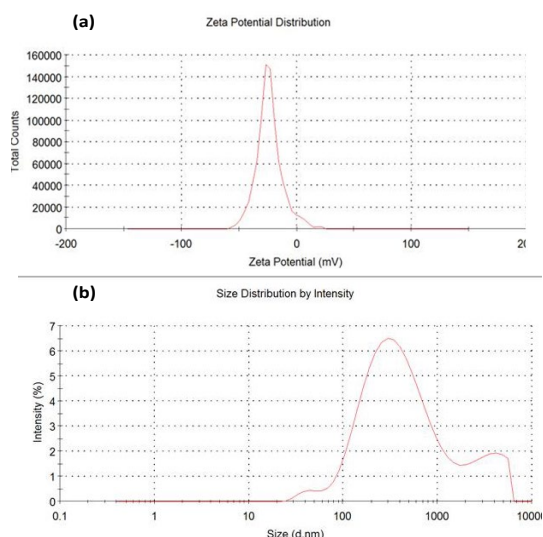


Figure 3: Zeta potential (a) and size distribution (b) of SS-ZnONPs sample

The FTIR analyses of silk sericin and SS- ZnONPs powders were given in Figure 4. In the FTIR result of pure silk sericin, amide I (at 1634 cm^{-1}), amide II (at 1515 cm^{-1}) and amide III (at 1236 cm^{-1}) peaks were clearly seen. In addition, the peaks around at 3266, 2927 and 1404 cm^{-1} were observed due to the O-H stretching vibration, C-H groups and symmetrical-asymmetrical stretching of the methyl group, respectively [5,7]. It was also observed that all peaks

belonging to sericin protein were present in the FTIR analysis of NPs. These findings proved that SS-ZnONPs were coated with sericin. Although there were peaks related to sericin in the spectrum of SS-ZnONPs compared to pure sericin, shifts in these peaks have occurred. These shifts resulted from the interaction of sericin with ZnO. Mumtaz et al. [40] synthesized ZnONPs using chitosan and silk fibroin, and by FTIR analysis, they observed that there were shifts in the peaks of chitosan and fibroin in the spectrum of coated ZnONPs. The authors attributed the reason for these shifts in the peaks to the interaction of chitosan and fibroin with ZnO. In the FTIR analysis of SS-ZnONPs, in addition to sericin-related peaks, a new peak observed at 618 cm^{-1} , which is the characteristic peak of the Zn-O band [41]. The formation of this peak proved the formation of ZnONPs in the presence of sericin as reducing agent. In addition, peaks associated with carboxylate ions (at 1593 cm^{-1}) and amine salt (at 847 cm^{-1}) were seen as the synthesis was performed in alkaline conditions using the sericin solution. These new peaks found in the SS-ZnONPs group represented that the amide bonds of silk sericin were hydrolyzed at alkaline conditions during the synthesis [5]. Moreover, in SS-ZnONPs FTIR result, a new peak formation observed at 1119 cm^{-1} indicated the presence of C-O around ZnONPs [42].

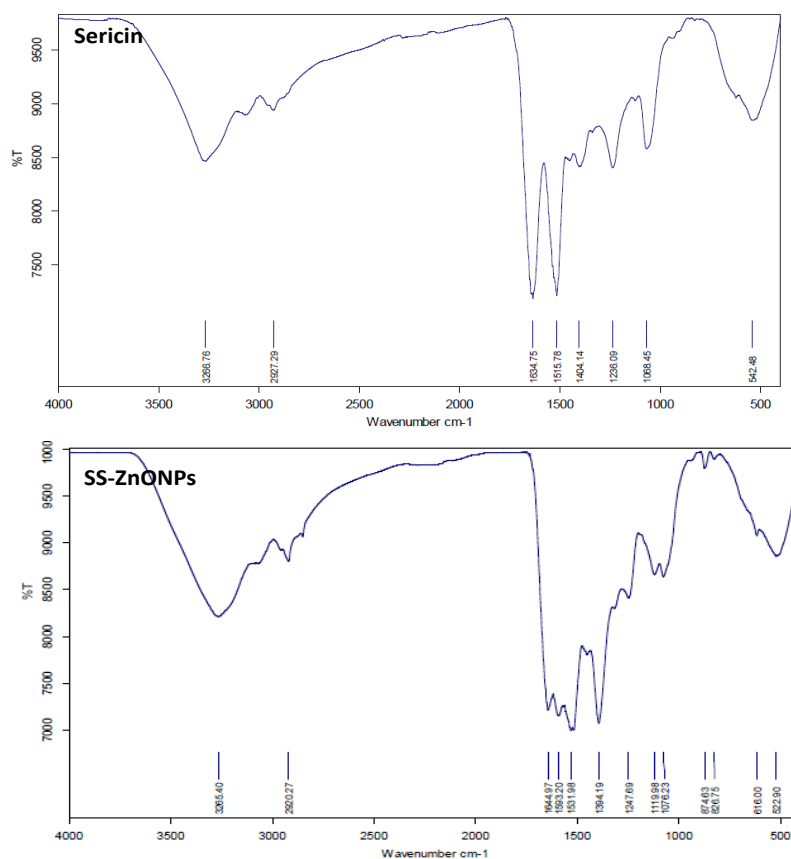


Figure 4: FTIR spectra of silk sericin and SS-ZnONPs sample

The SEM illustrations of SS-ZnONPs at different magnification were shown in Figure 5 (a) and (b). As seen from the images, the synthesized SS-ZnONPs have a cubic/hexagonal appearance and did not come together and form agglomerates. The high stability of particles with negative surface charge in zeta potential measurements has also been proven with SEM analysis. In addition, these images showed that by using silk sericin as a stabilizing and coating agent, NPs that were stable and did not form aggregates were obtained. In the literature, it has been shown that

stable ZnONPs were synthesized in ZnONPs synthesis studies using various substances as coating agents [33,34,40]. EDS analysis taken on the SEM pictures of SS-ZnONPs was given in Figure 5 (c). In the EDS analyses of SS-ZnONPs, peaks belonging to carbon, nitrogen, oxygen and sulfur elements as well as zinc peaks were observed. The existence of Zn peaks represented the formation ZnO from zinc salt. Due to the sericin protein, which was found as a coating agent around the obtained NPs, elemental structures belonging to the protein were seen in their structure.

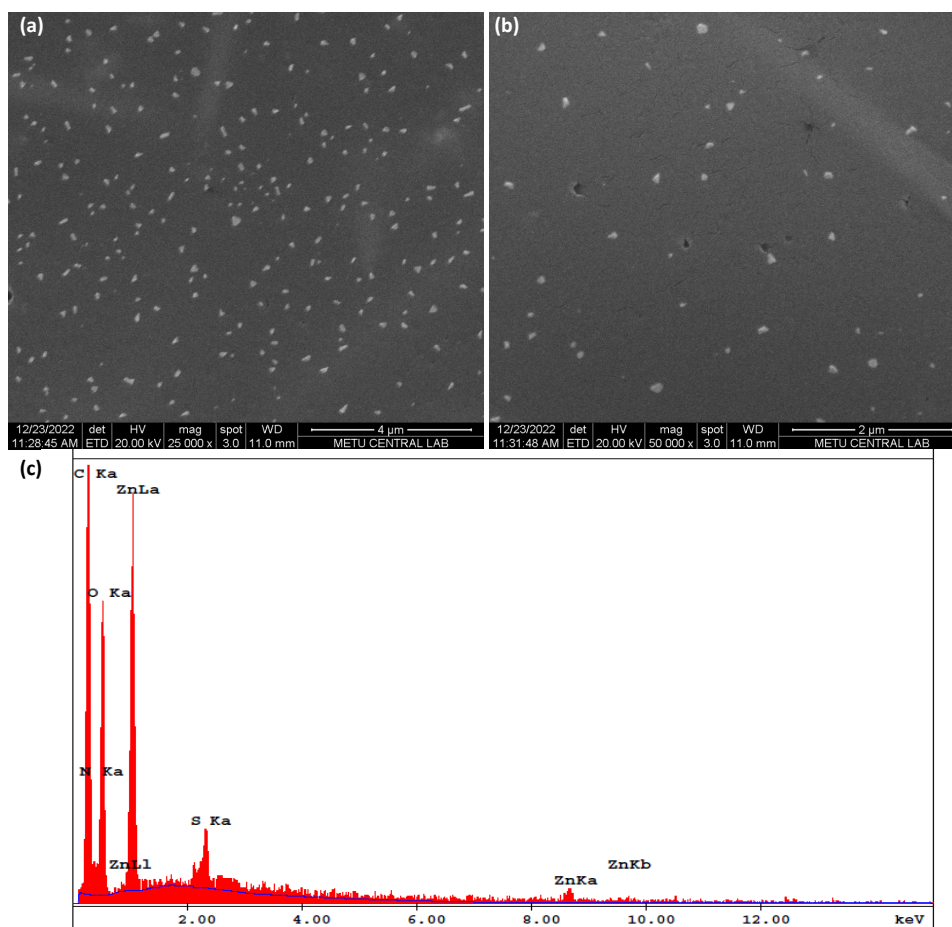


Figure 5: SEM images of SS-ZnONPs sample at different magnifications ((a) x25.000, (b) 50.000 magnification) and EDS analysis of SS-ZnONPs powder (c)

The XRD examination results of pure silk sericin and SS-ZnONPs were given in Figure 6. According to XRD result, sericin had contained both crystalline and amorphous structures. The sharp and wide peak, between 15-25°, showed the semi-crystalline structure of silk sericin with crystal and amorphous regions. In the XRD result of SS-ZnONPs, this broad peak belonging to the sericin was also found due to coating of ZnONPs with sericin. In ZnONPs synthesis studies

carried out with different coating agents, characteristic peaks belonging to the hexagonal structure of the ZnO formed have been reported in many previous studies [8,41]. As in these studies, in the XRD analysis of SS-ZnONPs, characteristic peaks of zinc oxide were found. The diffraction peaks found at 31.57, 34.032, 36.01, 47.515, 56.63, 62.68 and 67.83 ° associated with the 100, 002, 101, 102, 110, 103 and 112 hexagonal crystallographic planes of ZnO [42,43].

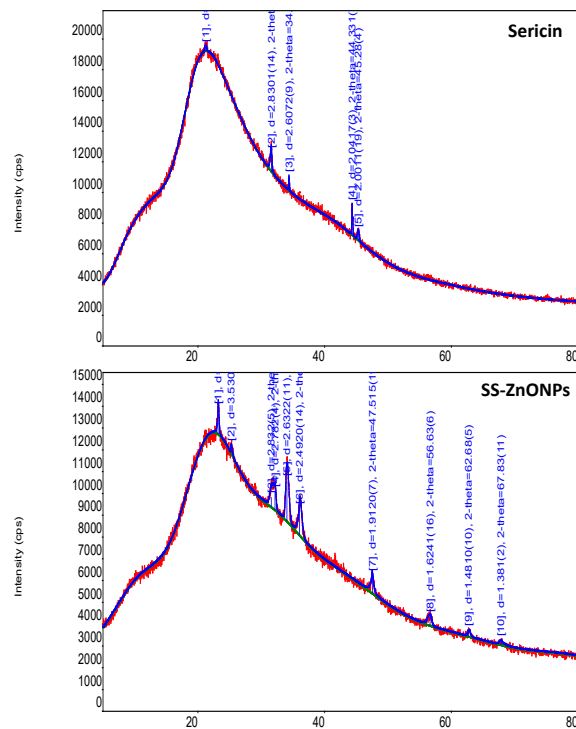


Figure 6: XRD spectra of silk sericin and SS-ZnONPs sample

The thermal degradation properties of pure silk sericin and SS-ZnONPs were investigated with TGA analysis and the results were given in Figure 7. According to TGA analysis, sericin degraded in 3 steps. In the first degradation step, sericin has lost moisture found its structure. In other degradation steps, organic structures of silk sericin were degraded [25] and the remaining mass of the silk sericin was found to be 20.276% at the end of 950 °C. According to TGA thermograms of SS-ZnONPs, SS-ZnONPs degraded in 4 steps. In the first step, it had lost the moisture in its structure, but the weight loss was more than the mass loss of silk sericin. ZnONPs are able to retain water in their structure and, compared to pure silk sericin, therefore, the mass loss due to moisture loss in the first step was increased. In the second and third degradations steps, the organic sections of silk sericin found around the ZnONPs degraded. In the 4th step, residual materials that may be on the surface of SS-ZnONPs have been degraded [44]. The amount remaining of SS-ZnONPs was found to be 29.922% at 950 °C. TGA analysis results showed that the amount of remaining substance in ZnONPs samples increased at 950 °C in comparison with pure sericin. The increment in the amount of remaining residue compared to the pure sericin was due to the formation of ZnONPs.

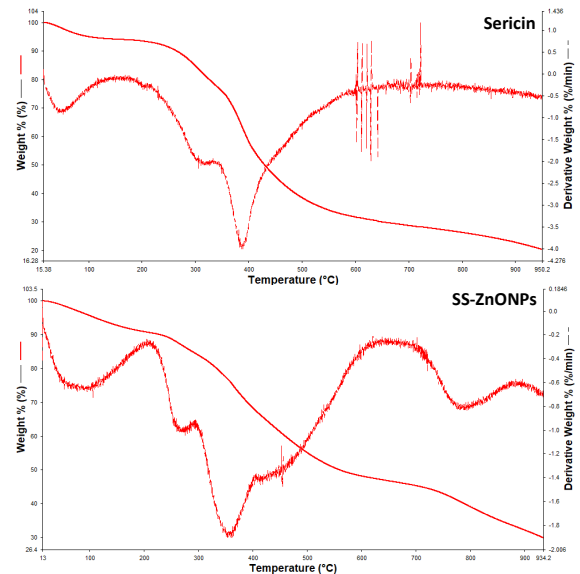


Figure 7: TGA results of silk sericin and SS-ZnONPs powder

3.3. Antibacterial Properties of SS-ZnONPs

NPs are seen as substitutes for antibiotics due to their low toxicity to the human body and broad-spectrum lethal effects against pathogenic microorganisms [45,46]. Bacterial cell walls are negatively charged because of teichoic acid found in gram-positive and phospholipid found in gram-negative bacteria. Therefore, it is thought that the ions released from NPs interact with the negatively charged cell wall and NPs show antibacterial activity [2,8]. The antimicrobial effects of NPs can be determined by growing microorganisms in culture media containing NPs or by establishing a direct interaction medium by electrospinning [47,48].

Bacteria are divided into two main groups, gram positive and gram negative, according to differences in their cell wall structures. The cell wall differences of gram-positive and gram-negative bacteria create differences in the behaviour of bacteria against antibacterial materials [32]. In our study, in antibacterial test, we used *S. aureus* bacteria as gram-positive bacteria and *E. coli* bacteria as gram-negative bacteria, which are frequently used in antibacterial tests.

There are studies showing that ZnONPs synthesized with different coating agents have antibacterial activity on many microorganisms [40,49,50]. In the present study, antibacterial properties of the produced SS-ZnONPs was investigated against gram-positive *S. aureus* and gram-negative *E. coli* with performed agar well-diffusion test. The measured inhibition diameters for the samples and agar images of test were represented in Table 1 and Figure 8, respectively. For *E. coli*, it was observed that no zones of inhibition were formed around the wells in which SS-ZnONPs were added. These results showed that the obtained NPs did not show any antibacterial effect on *E. coli*,

which is in the gram-negative bacteria. In addition, in experiments with *S. aureus*, inhibition zones were found around the wells and this result showed that SS-ZnONPs have antibacterial activities for *S. aureus*. Previous studies have shown that ZnONPs own more lethal influence on gram-positive bacteria [51,52].

This is an acceptable result, because, in general, gram-negative bacteria show high resistance to antibacterial agents compared to gram-positive bacteria, due to the outer membrane structure found in their cell walls [32].

Table 1. Measured inhibition zone values for positive, negative control, and SS-ZnONPs sample

Samples	Zone of Inhibition for <i>E. coli</i> (mm)	Zone of Inhibition for <i>S. aureus</i> (mm)
Posicitive control (PC, Gentamicin,10 µg)	19.67±0.41	22.67±0.82
Negative control (NC, sterilized water)	0	0
SS-ZnONPs	0	12.42±0.33

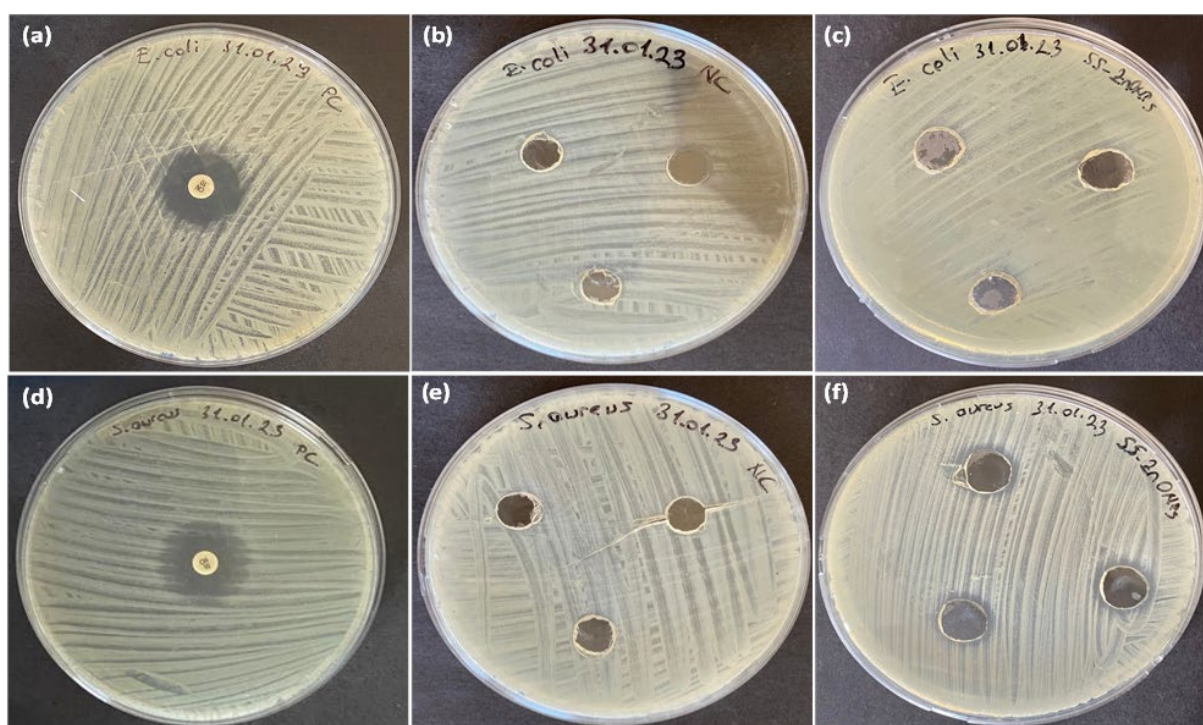


Figure 8: Agar images of the applied antibacterial test (for *E. coli*; positive control (a), negative control (b), SS-ZnONPs sample (c), for *S. aureus* positive control (a), negative control (b), SS-ZnONPs sample (c)).

IV. CONCLUSIONS

In the current work, green synthesis method was applied for producing of SS-ZnONPs. The synthesis of the obtained SS-ZnONPs was confirmed both by colour change and UV-Vis analysis. The chemical feature of the obtained SS-ZnONPs were examined by FTIR, and the Zn-O peak formed in the FTIR analysis was shown chemically to form ZnONPs. Looking at the SEM photographs, it is understood that the synthesized NPs have a cubic/hexagonal appearance and did not come together and form agglomerates. EDS analysis performed on SEM photographs showed that there were oxygen, carbon, sulphur, and nitrogen peaks in the structure of NPs, originating from the

coating agent sericin. Moreover, Zn peak was seen in EDS analysis and this result proved that the elemental form of Zn was formed. In XRD analysis, crystallographic peaks belonging to the hexagonal structure of Zn were observed. With TGA analysis, it was observed that, compared to the pure sericin, there was an increase in the amount of remaining mass of SS-ZnONPs without degradation at the end of 950 °C due to the formation of Zn-O. Finally, it was confirmed that the synthesized NPs had an antibacterial effect on *S. aureus*, a gram-positive bacterium.

ACKNOWLEDGMENTS

This study was carried out at Kırıkkale University. We would like to thank Kırıkkale University for providing us with every opportunity to carry out our study.

REFERENCES

- [1] Railean-Plugaru, V., Pomastowski, P., Wypij, M., Szultka-Mlynska, M., Rafinska, K., Golinska, P., Dahm, H., Buszewski, B. (2016). Study of silver NPs synthesized by acidophilic strain of Actinobacteria isolated from the of *Picea sitchensis* forest soil. *J. Appl. Microbiol.*, 120, 1250-1263. <https://doi.org/10.1111/jam.13093>
- [2] Krol, A., Pomastowski, P., Rafinska, K., Railean-Plugaru, V., Buszewski, B. (2017) Zinc oxide NPs: Synthesis, antiseptic activity and toxicity mechanism. *Adv. Colloid Interface Sci.*, 249, 37-52. <https://doi.org/10.1016/j.cis.2017.07.033>
- [3] Buzea, C., Pacheco, I.I., Robbie, K. (2007) Nanomaterials and NPs: sources and toxicity. *Biointerphases*, 2, 17-71. <https://doi.org/10.1116/1.2815690>
- [4] Jayachandran, A., Aswathy. T.R., Achuthsankar, S.N. (2021) Green synthesis and characterization of zinc oxide NPs using *Cayratia pedata* leaf extract. *Biochem. Biophys. Rep.*, 26, 100995. <https://doi.org/10.1016/j.bbrep.2021.100995>
- [5] Gün Gök, Z., Günay, K., Arslan, M., Yiğitoğlu, M., Vargel, İ. (2020) Coating of modified poly(ethylene terephthalate) fibers with sericin-capped silver NPs for antimicrobial application. *Polym. Bull.*, 77, 649-1665. <https://doi.org/10.1007/s00289-019-02820-0>
- [6] Bozkaya, O., Arat, E., Gün Gök, Z., Yiğitoğlu, M., Vargel, İ. (2022) Production and characterization of hybrid nanofiber wound dressing containing *Centella asiatica* coated silver NPs by mutual electrospinning method. *Eur. Polym. J.*, 166, 111023. <https://doi.org/10.1016/j.eurpolymj.2022.111023>
- [7] Gün Gök, Z. (2022), Synthesis and characterization of polyvinyl alcohol-silk sericin nanofibers containing gelatin-capped silver NPs for antibacterial applications. *Polym. Bull.*, 79, 10357-10376. <https://doi.org/10.1007/s00289-022-04455-0>
- [8] Chauhan, N., Thakur, B., Kumari, A., Khatana, C., Sharma, R. (2023) Mushroom and silk sericin extract mediated ZnONPs for removal of organic pollutants and microorganisms. *S. Afr. J. Bot.*, 153, 370-381. <https://doi.org/10.1016/j.sajb.2023.01.001>
- [9] Sadhasivam, S., Shanmugam, M., Umamaheswaran, P.D., Venkattappan, A., Shanmugam, A. (2021) Zinc Oxide NPs: Green Synthesis and Biomedical Applications. *J. Clust. Sci.*, 32, 1441-1455. <https://doi.org/10.1007/s10876-020-01918-0>
- [10] Tapiero, H., Tew, K.D. (2003) Trace elements in human physiology and pathology: zinc and metallothioneins. *Biomed Pharmacother.*, 57, 299-411 (2003). [https://doi.org/10.1016/s0753-3322\(03\)00081-7](https://doi.org/10.1016/s0753-3322(03)00081-7)
- [11] Dulta, K., Koşarsoy Ağçeli, G., Chauhan, P., Jasrotia, R., Chauhan, P.K. (2021) A Novel Approach of Synthesis Zinc Oxide NPs by *Bergenia ciliata Rhizome* Extract: Antibacterial and Anticancer Potential. *J. Inorg. Organomet. Polym. Mater.*, 31, 180-190. <https://doi.org/10.1007/s10904-020-01684-6>
- [12] Calestani, D., Zha, M., Mosca, R., Zappettini, A., Carotta, M.C., Di Natale, V., Zanotti, L. (2010) Growth of ZnO tetrapods for nanostructure-based gas sensors. *Sens. Actuators B*, 144(2), 472-478. <https://doi.org/10.1016/j.snb.2009.11.009>
- [13] Mandal, A.K., Katuwal, S., Tettey, F., Gupta, A., Bhattarai, S., Jaisi, S., Bhandari, D.P., Shah, A.K., Bhattarai, N., Parajuli, N. (2022) Current Research on Zinc Oxide NPs: Synthesis, Characterization, and Biomedical Applications. *Nanomaterials*, 12, 3066. <https://doi.org/10.3390/nano12173066>
- [14] Aramwit, P., Siritientong, T., Srichana, T. (2012) Potential applications of silk sericin, a natural protein from textile industry by-products. *Waste Manag. Res.*, 30, 212-224. <https://doi.org/10.1177/0734242X11404733>
- [15] Akturk, O., Kismet, K., Yasti, A.C., Kuru, S., Duymus, M.E., Kaya, F., Caydere, M., Hucumenoglu, D., Keskin, D. (2016) Wet electrospun silk fibroin/gold nanoparticle 3D matrices for wound healing applications. *RSC Adv.*, 6, 13234-13250. <https://doi.org/10.1039/C5RA24225H>
- [16] Aramwit, P., Keongamaroon, O., Siritientong, T., Bang, N., Supasynhdh, O. (2012) Sericin cream reduces pruritus in hemodialysis patients: a randomized, double-blind, placebo-controlled experimental study. *BMC Nephrol.*, 13, 119. <https://doi.org/10.1186/1471-2369-13-119>
- [17] Yang, M., Mandal, N., Shuai, Y., Zhou, G., Min, S., Zhu, L. (2014) Mineralization and Biocompatibility of *Antheraea pernyi* (A. pernyi) Silk Sericin Film for Potential Bone Tissue Engineering. *Bio-Med. Mater. Eng.*, 24, 815-824 (2014). <https://doi.org/10.3233/bme-130873>
- [18] Tao, G., Cai, R., Wang, Y., Liu, L., Zuo, H., Zhao, P., Umar, A., Mao, C., Xia, Q., He, H. (2019) Bioinspired design of AgNPs embedded silk sericin-based sponges for efficiently combating bacteria and promoting wound healing. *Mater. Des.*, 180, 107940. <https://doi.org/10.1016/j.matdes.2019.107940>
- [19] Liu, L., Cai, R., Wang, Y., Tao, G., Ai, L., Wang, P., Yang, M., Zuo, H., Zhao, P., He, H. (2018) Polydopamine-Assisted Silver Nanoparticle Self-Assembly on Sericin/Agar Film for Potential Wound Dressing Application. *Int. J.*

- Mol. Sci., 19(10), 2875. <https://doi.org/10.3390%2Fijms19102875>
- [20] Li, X., Hou, S., Chen, J., He, C.E., Gao, Y.E., Lu, Y., Jia, D., Ma, X., Xue, P., Kang, Y. (2021) Engineering silk sericin decorated zeolitic imidazolate framework-8 nanoplatfrom to enhance chemotherapy. *Colloids Surf. B*, 200, 111594. <https://doi.org/10.1016/j.colsurfb.2021.111594>
- [21] Zhang, Y., Liu, J., Huang, L., Wang, Z., Wang, L. (2015) Design and performance of a sericin alginate interpenetrating network hydrogel for cell and drug delivery. *Sci. Rep.*, 5, 12374. <https://doi.org/10.1038/srep12374>
- [22] Sheng, J.Y., Xu, J., Zhuang, Y., Sun, D.Q., Xing, T.L., Chen, G.Q. (2013) Study on the application of sericin in cosmetics. *Adv. Mater. Res.*, 796, 416-423. <https://doi.org/10.4028/www.scientific.net/AMR.796.416>
- [23] Padamwar, M.N., Pawar, A.P., Daithankar, A.V., Mahadik, K. (2005) Silk sericin as a moisturizer: an *in vivo* study. *J. Cosmet. Dermatol.*, 4(4), 250-257. <https://doi.org/10.1111/j.1473-2165.2005.00200.x>
- [24] Takechi, T., Takamura, H. (2014) Development of bread supplemented with the silk protein sericin. *Food Sci. Technol. Res.*, 20(5), 1021-1026. <https://doi.org/10.3136/fstr.20.1021>
- [25] Gün Gök, Z., Yiğitoğlu, M., Vargel, İ., Sahin, Y., Alçıgır, M.E. (2021) Synthesis, characterization and wound healing ability of PET based nanofiber dressing material coated with silk sericin capped-silver NPs. *Mater. Chem. Phys.*, 259, 124043. <https://doi.org/10.1016/j.matchemphys.2020.124043>
- [26] Akturk, O., Gün Gök, Z., Erdemli, Ö., Yiğitoğlu, M. (2019) One-pot facile synthesis of silk sericin-capped gold NPs by UVC radiation: investigation of stability, biocompatibility, and antibacterial activity. *J. Biomed. Mater. Res.*, 107A, 2667-2679. <https://doi.org/10.1002/jbm.a.36771>
- [27] Akturk, O., Gün Gök, Z., Daş, M.T., Erdemli, Ö. (2018) Synthesis and characterization of sericin-capped gold NPs. *J. Fac. Eng. Archit. Gazi Univ.*, 33, 675-684. <https://doi.org/10.17341/gazimmfd.416377>
- [28] Aramwit, P., Bang, N., Ratanavaraporn, J., Ekgasit, S. (2014) Green synthesis of silk sericin-capped silver NPs and their potent anti-bacterial activity. *Nanoscale Res. Lett.*, 9, 79-86 (2014). <https://doi.org/10.1186/1556-276X-9-79>
- [29] Purwar, R., Sharma, S., Sahoo, P., Srivastava, C.M. (2015) Flexible sericin/polyvinyl alcohol/clay blend films. *Fibers Polym.*, 16, 761-768. <https://doi.org/10.1007/s12221-015-0761-y>
- [30] Kwak, H.W., Lee, K.H. (2018) Polyethylenimine-functionalized silk sericin beads for high-performance remediation of hexavalent chromium from aqueous solution. *Chemosphere*, 207, 507-516. <https://doi.org/10.1016/j.chemosphere.2018.04.158>
- [31] Chuang, C.C., Prasanna, A., Huang, B.R., Hong, P.D., Chiang, M.Y. (2017). Simple synthesis of eco-friendly multifunctional silk-sericin capped zinc oxide nanorods and their potential for fabrication of hydrogen sensors and UV photodetectors. *ACS Sustain. Chem. Eng.* 5(5), 4002-4010. <https://doi.org/10.1021/acssuschemeng.7b00012>
- [32] Gün Gök, Z., Karayel, M., Yiğitoğlu, M. (2021) Synthesis of carrageenan coated silver NPs by an easy green method and their characterization and antimicrobial activities. *Res. Chem. Intermed.*, 47, 1843-1864. <https://doi.org/10.1007/s11164-021-04399-6>
- [33] Santhoshkumar, J., Kumar, S.V., Rajeshkumar, S. (2017) Synthesis of zinc oxide nanoparticles using plant leaf extract against urinary tract infection pathogen. *Resour.-Effic. Technol.*, 3(4), 459-465. <https://doi.org/10.1016/j.reffit.2017.05.001>
- [34] Suresh, D., Nethravathi, P.C., Rajanaika, H., Nagabhushana, H., Sharma, S.C. (2015) Green synthesis of multifunctional zinc oxide (ZnO) nanoparticles using *Cassia fistula* plant extract and their photodegradative, antioxidant and antibacterial activities. *Mater. Sci. Semicond. Process.*, 31, 446-454. <https://doi.org/10.1016/j.mssp.2014.12.023>
- [35] Rajapriya, M., Sharmili, S.A., Baskar, R., Balaji, R., Alharbi, N.S., Kadaikunnan, S., Khaled, J.M., Alanzi, K.F., Vaseeharan, B. (2020) Synthesis and characterization of zinc oxide nanoparticles using *Cynara scolymus* Leaves: Enhanced hemolytic, antimicrobial, antiproliferative, and photocatalytic activity. *J. Cluster Sci.*, 31, 791-801. <https://doi.org/10.1007/s10876-019-01686-6>
- [36] Karthik, S., Siva, P., Balu, K.S., Suriyaprabha, R., Rajendran, V., Maaza, M. (2017) Acalypha indica-mediated green synthesis of ZnO nanostructures under differential thermal treatment: Effect on textile coating, hydrophobicity, UV resistance, and antibacterial activity. *Adv. Powder Technol.*, 28(12), 3184-3194. <https://doi.org/10.1016/j.apt.2017.09.033>
- [37] Wooten, A.J., Werder, D.J., Williams, D.J., Casson, J.L., Hollingsworth, J.A. (2009) Solution-liquid-solid growth of ternary Cu-In-Se semiconductor nanowires from multiple- and single-source precursors. *J. Am. Chem. Soc.*, 131, 16177-1618. <https://doi.org/10.1021/ja905730n>
- [38] Pudukudy, M., Yaakob, Z. (2015) Facile Synthesis of Quasi Spherical ZnO NPs with Excellent Photocatalytic Activity. *J. Clust. Sci.*, 26, 1187-1201. <https://doi.org/10.1007/s10876-014-0806-1>
- [39] Farhadi, S., Ajerloo, B., Mohammadi, A. (2017) Green Biosynthesis of Spherical Silver NPs by

- Using Date Palm (*Phoenix Dactylifera*) Fruit Extract and Study of Their Antibacterial and Catalytic Activities. *Acta. Chim. Slov.*, 64, 129-143. <https://doi.org/10.17344/acs.2016.2956>
- [40] Mumtaz, S., Ali, S., Tahir, H.M., Mumtaz, S., Mughal, T.A., Kazmi, S.A.R., Hassan, A., Summer, M., Zulfiqar, A., Kazmi, S. (2024) Biological applications of biogenic silk fibroin–chitosan blend zinc oxide nanoparticles. *Polym. Bull.*, 81, 2933-2956. <https://doi.org/10.1007/s00289-023-04865-8>
- [41] Patrón-Romero, L., Luque, P.A., Soto-Robles, C.A., Nava, O., Vilchis-Nestor, A.R., Barajas-Carrillo, V.W., Martínez-Ramírez, C.E., Chávez Méndez, J.R., Alvelais Palacios, J.A., Leal Ávila, M.A., Almanza-Reyes, H. (2020) Synthesis, characterization and cytotoxicity of zinc oxide NPs by green synthesis method. *J. Drug Deliv. Sci. Technol.*, 60, 101925. <https://doi.org/10.1016/j.jddst.2020.101925>
- [42] Indubala, E., Dhanasekar, M., Sudha, V., Padma Malar, E.J., Divya, P., Sherine, J., Rajagopal, R., Bhat, S.V., Harinipriya, S. (2018) l-Alanine capping of ZnO nanorods: increased carrier concentration in ZnO/CuI heterojunction diode. *RSC Adv.*, 8, 5350-5361. <https://doi.org/10.1039/C7RA12385J>
- [43] Stankovic' A., Dimitrijevic', S., Uskokovic', D. (2013) Influence of size scale and morphology on antibacterial properties of ZnO powders hydrothermally synthesized using different surface stabilizing agents. *Colloids Surf., B*, 102, 21-28. <https://doi.org/10.1016/j.colsurfb.2012.07.033>
- [44] Menazea, A.A., Ismail, A.M., Samy, A. (2021) Novel Green Synthesis of Zinc Oxide NPs Using Orange Waste and Its Thermal and Antibacterial Activity. *J. Inorg. Organomet. Polym. Mater.*, 31, 4250-4259. <https://doi.org/10.1007/s10904-021-02074-2>
- [45] Maleki Dizaj, S., Mennati, A., Jafari, S., Khezri, K., Adibkia, K. (2015) Antimicrobial Activity of Carbon-Based NPs. *Adv. Pharm. Bull.*, 5, 19-23. <https://doi.org/10.5681/apb.2015.003>
- [46] Akbar, S., Tauseef, I., Subhan, H., Sultana, N., Khan, I., Ahmed, U., Syed Haleem, K. (2020) An overview of the plant-mediated synthesis of zinc oxide NPs and their antimicrobial potential. *Inorg. Nano-Met. Chem.*, 50, 257-271. <https://doi.org/10.1080/24701556.2019.1711121>
- [47] Rana, S., Kalaichelvan, P. (2011) Antibacterial Activities of Metal NPs. *Adv. Bio. Tech.*, 11, 21-23.
- [48] Yamamoto, O. (2001) Influence of particle size on the antibacterial activity of zinc oxide. *Int. J. Inorg. Mater.*, 3, 643-646. [https://doi.org/10.1016/S1466-6049\(01\)00197-0](https://doi.org/10.1016/S1466-6049(01)00197-0)
- [49] Wahab, R., Siddiqui, M.A., Saquib, Q., Dwivedi, S., Ahmad, J., Musarrat, J., Al-Khedhairi, A.A., Shin, H.-S. (2014) ZnO nanoparticles induced oxidative stress and apoptosis in HepG2 and MCF-7 cancer cells and their antibacterial activity. *Colloids Surf., B*, 117, 267-276. <https://doi.org/10.1016/j.colsurfb.2014.02.038>
- [50] Babayevska, N., Przysiecka, Ł., Iatsunskyi, I., Nowaczyk, G., Jarek, M., Janiszewska, E., Jurga, S. (2022) ZnO size and shape effect on antibacterial activity and cytotoxicity profile. *Scientific Reports*, 12(1), 8148. <https://doi.org/10.1038/s41598-022-12134-3>
- [51] Yusof, N.A.A., Zain, N.M., Pauzi, N. (2019) Synthesis of ZnO nanoparticles with chitosan as stabilizing agent and their antibacterial properties against Gram-positive and Gram-negative bacteria. *Int. J. Biol. Macromol.*, 124, 1132-1136. <https://doi.org/10.1016/j.ijbiomac.2018.11.228>
- [52] Yu, Y.C., Hu, M.H., Zhuang, H.Z., Phan, T.H.M., Jiang, Y.S., Jan, J.S. (2023) Antibacterial Gelatin Composite Hydrogels Comprised of In Situ Formed Zinc Oxide Nanoparticles. *Polymers*, 15(19), 3978. <https://doi.org/10.3390/polym15193978>